

pubs.acs.org/JPCC Article

Deformed Butler-Volmer Models for Convex Semilogarithmic Current-Overpotential Profiles of Li-ion Batteries

Anis Allagui,* Hachemi Benaoum, and Chunlei Wang



Cite This: J. Phys. Chem. C 2022, 126, 3029-3036

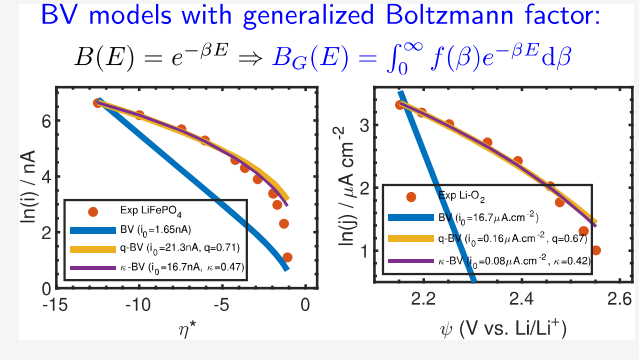


ACCESS |

Metrics & More

Article Recommendations

ABSTRACT: The Butler–Volmer (BV) equation links the current flux crossing an electrochemical interface to the electric potential drop across it with the assumption of Arrhenius kinetics and the Boltzmann factor. Applying the semilogarithmic Tafel analysis in which the logarithm of current is plotted vs the overpotential, one expects straight lines from which the fundamental reaction rate of the kinetic process can be computed. However, some Li-ion battery data, which is the focus here, show nonlinear convex profiles that cannot be adequately fitted with the standard BV model. We propose instead two deformed BV models for the analysis of such types of behaviors constructed from the superposition of cells exhibiting only local equilibrium and thus giving rise to the power-law q-exponential and κ -exponential functions. Non-Boltzmann distributions have been



successfully employed for the modeling of a wide spectrum of physical systems in nonequilibrium situations, but not yet for batteries. We verify the validity of the deformed BV models on experimental data obtained from $LiFePO_4$ and $Li-O_2$ batteries.

■ INTRODUCTION

Chemical-to-electrical or electrical-to-chemical energy conversion in electrochemical energy devices and systems such as batteries and fuel cells or in electrodeposition and electrolysis require the presence of two phases in contact with each other. Generally there is an electron-conducting phase but ionic insulator on one hand and an ionic conductor but electric insulator on the other hand. The phases can be solid, liquid, or gas. At the interphase boundary or interface, which should be thought of as a physical and not a mathematical plane, chemical reactions accompanied by charge carrier transfers from one phase to another take place. Understanding and properly modeling the measurements carried out on such systems is important for many applications including renewable energy technologies with energy storage, electric vehicles, smart grids, and corrosion prevention. In particular, it is important and useful to describe the system-level relationship between the electrical current flowing through an electrode, or charge dynamics with time, and the potential difference between the electrode itself and a point in the bulk electrolyte. Several approaches have been proposed to model kinetic rate behavior. The macroscopic phenomenological Butler-Volmer (BV) model is the de facto mathematical model used for describing the simultaneous anodic reaction (oxidation) and cathodic reaction (reduction) on the same electrode surface.2 Microscopic theories, including Marcus, Marcus-Hush (MH), Marcus-Hush-Chidsey (MHC), and their extensions, are also powerful in describing electron transfer kinetics in both

directions but also with physically tractable quantities.^{3–5} However, the main limitation for the widespread use of Marcus-type theories is probably that the rate at metal electrodes/electrolyte has no simple closed-form expression as it is defined in terms of indefinite integral of a Gaussian function (classical Marcus rate for the transfer of an electron) over Fermi–Dirac distribution of electrons.⁶ Different computational algorithms have been proposed with different levels of accuracy and computational costs.⁷ There are also a few simple and other more cumbersome approximating formulas that have been derived and verified.^{5,6,8–10}

Our focus in this study is on the BV formalism and ways to extend its application to nonequilibrium steady-state systems using the concepts of superstatistics^{11–13} as we shall show below. First, let us recall that the BV equation can be derived from different approaches including the kinetic law of mass action, ¹⁴ nonequilibrium thermodynamics, ² principle of thermal activation process, ¹⁵ and also first-principles, ¹⁶ but here we present the derivation from transition state theory. ¹⁷ From Arrhenius kinetics, it is observed that the natural logarithm of the reaction

Received: November 7, 2021 Revised: January 12, 2022 Published: February 8, 2022





rate k and the reciprocal of the absolute temperature T are linearly related according to

$$\frac{\partial \ln(k)}{\partial (1/T)} = -\frac{E_{\rm a}}{R} \tag{1}$$

where R is the universal gas constant and $E_{\rm a}$ is an experimental/phenomenological activation energy, ¹⁴ which can be thought of as the energy necessary to overcome a certain energy barrier for particles to transition from the well of reactants to the well of products, and thus for the reaction to proceed. Arrhenius' suggestion that there is a transition state intermediate between reactants and products was central to the development of transition state theory. ¹⁸ Let us consider the case of a single-step charge transfer redox reaction of the form:

$$Ox + ne^- \rightleftharpoons Red$$
 (2)

The forward or oxidation $(Ox + ne^- \rightarrow Red)$ and backward or reduction $(Red \rightarrow Ox + ne^-)$ charge transfer reactions can be described by the charge transfer reaction rates $k_{\rm f}$ and $k_{\rm b}$. Their associate forward and backward current densities (per unit surface) crossing the interface are taken to be proportional to the surface concentrations $C_{\rm Ox}$ and $C_{\rm Red}$ and can be written as

$$i_{\rm f} = nFk_{\rm f}C_{\rm Ox} \tag{3}$$

$$i_{\rm b} = nFk_{\rm b}C_{\rm Red} \tag{4}$$

where F is the Faraday constant. Thus, the net current flowing through the electrode is given by the difference: 14

$$i = i_{\rm f} - i_{\rm b} = nF(k_{\rm f}C_{\rm Ox} - k_{\rm b}C_{\rm Red}) \tag{5}$$

Now by incorporating the expressions for the potential and temperature-dependence of the forward and backward charge transfer reaction rates, which are assumed to follow Arrhenius profiles (with E_a taken as a linear function of the potential ψ) as

$$k_{\rm f} = k_{\rm f}^{\,0} \, \exp\!\left(\frac{-\alpha_{\rm Red} \psi}{RT/F}\right) \tag{6}$$

$$k_{\rm b} = k_{\rm b}^0 \exp\left(\frac{\alpha_{\rm Ox} \psi}{RT/F}\right) \tag{7}$$

Equation 5 turns out to be

$$i = nF \left\{ k_{\rm f}^{\,0} C_{\rm Ox} \, \exp \left(\frac{-\alpha_{\rm Red} \psi}{RT/F} \right) - k_{\rm b}^{\,0} C_{\rm Red} \, \exp \left(\frac{\alpha_{\rm Ox} \psi}{RT/F} \right) \right\}$$
(8)

This equation is known as the kinetic BV equation for the current—potential relationship with pure charge transfer overpotential. Here, the dimensionless parameters $\alpha_{\rm Red}$ and $\alpha_{\rm Ox}$ (taking values between 0 and 1 with $\alpha_{\rm Red} + \alpha_{\rm Ox} = 1$) denote the transfer or symmetry factors associated with the oxidation and reduction reactions, respectively, or qualitatively a measure of the "position" of the transition state, 19 $RT/F = V_{\rm th}$ is the thermal voltage, and ψ is the potential of the electrode through which current flows, which is different from the equilibrium potential ψ_0 established when no current passes through the electrode. The difference $\eta = \psi - \psi_0$ is known as the overpotential. Equation 8 can also be expressed in terms of the current exchange density i_0 (i.e., when $i_f = i_b = i_0$ which takes place at the equilibrium potential ψ_0) such that

$$i = i_0 \left\{ \exp\left(\frac{-\alpha_{\text{Red}}\eta}{RT/F}\right) - \exp\left(\frac{\alpha_{\text{Ox}}\eta}{RT/F}\right) \right\}$$
(9)

Note that with the use of the dimensionless overpotential scaled to the thermal voltage, $\eta^* = \eta/V_{\text{th}}$, the dimensionless current $i^* = i/i_0$, and $\alpha_{\text{Red}} = \alpha$, eq 9 can be rewritten as 1

$$i^* = \exp[-\alpha \eta^*] - \exp[(1 - \alpha)\eta^*]$$
 (10)

For the particular case of α = 0.5, which is commonly used for battery modeling, the expression for i^* simplifies to

$$i^* = 2 \sinh(-\eta^*/2)$$
 (11)

The Tafel technique of plotting $\ln(i^*)$ versus η^* gives a straight line of slope $-\alpha$ for $\eta^* < 0$ and $(1 - \alpha)$ for $\eta^* > 0$ from which the charge transfer rates can be estimated. 1,20-22

The validity of the BV model is based on the assumption that the concentration of the reacting species are independent of the current density and the potential, and consequently only pure charge transfer overpotential is involved. 17 It is also commonly assumed that the transfer coefficient is independent or a weak function of the applied potential and can be considered as constant. 19 The surface of the electrode is considered flat and stress-free. 15 Furthermore, within the BV framework an exponential Boltzmann factor for the reaction rate dependence on the temperature is considered. The Boltzmann factor, which is essentially a comparison between the energy of the molecules and the energy of the barrier when the system is in thermodynamic equilibrium and characterized by a certain temperature, assumes that particles are totally independent and non-interacting and obey the laws of ideal gases.²³ It also assumes that elementary volumes of the system are equiprobable. These assumptions are the basis for Boltzmann-Gibbs (BG) statistical mechanics in which the exponential and Gaussian distributions are those that maximize the BG entropy by virtue of the Central Limit Theorem (CLT) and ensure the equilibrium state.

However, there are several instances where the semilogarithmic Tafel analysis of $ln(i^*)$ versus η^* does not result in linear profiles, but rather curved plots, which is the motivation for this work. 1,21,22,24-26 Focusing on battery materials and devices, curved Tafel plots have been reported, for instance, by Munakata et al. 25 in experiments conducted on single (porous) particles of LiFePO₄, which is a widely used cathode material for large-scale batteries. The fitting with the BV model with the symmetry factor $\alpha = 0.5$ was reasonable enough for a small portion of the voltage—current data only. 25 Viswanathan et al. 26 also reported highly nonlinear Tafel plots for the discharge of a nonaqueous Li-air (or Li-O₂) battery. The charging data were less unusual by showing slight nonlinearities in the profiles. Generally speaking, reaction systems we are interested in are actually away from equilibrium and transition from one metastable state to a neighboring state of metastable equilibrium in response to external stimuli.²⁷ Thus, the assumption of thermodynamic equilibrium is not always appropriate, and the statistics may not necessarily follow BG statistics. 18,23,27 In fact, for many complex systems at off-equilibrium conditions it is often observed that power-law distributions are most common, as is the case, for example, with the dissolution reaction of magnesium (or aluminum) in aqueous cupric chloride solution.²⁸ Magnesium (or aluminum) dissolves to form MgCl₂ (or AlCl₃), and copper precipitates at local reaction rates that can be affected by concentration fluctuations, pitting dissolution and the formation of the Cu layer, which tends to inhibit the reaction itself. Furthermore, the breakdown of the Cu layer because of liberation of hydrogen gas, convective turbulence near the reactive surface, and erosion of underlying

metal increases the local reaction rate at the freshly exposed surfaces. As a result, one observes fluctuations in current and voltage found to follow power-law behavior. Other systems that exhibit power-law statistics are, for example, the power grid frequency fluctuations, epidemiology and spreading dynamics of diseases, and atomic packing in metallic glasses, to name a few.

The purpose of this contribution is to formulate and study generalized BV models by incorporating the power-law (i) qexponential function based on Tsallis nonextensive statistics² and (ii) the κ -exponential based on Kaniadakis statistics 34,35 instead of the traditional exponential Boltzmann factor based on BG statistics. Such approaches have been proven successful for describing many complex nonequilibrium systems at the stationary state that behave like the collective superposition of many subsystems, themselves following the BG statistics. These systems usually involve long-range interactions, non-Markovian memory effects, and anomalous diffusion, for instance.³⁶ The single Boltzmann factor employed in the BV kinetic model is recovered as a limiting case. We note that the generalization of reaction rate coefficients using the q-exponential structure instead of the standard exponential function has been proposed by Niven,³⁷ Bagci,³⁸ and Yin et al.,^{39–41} among others,^{42–45} but to the best of our knowledge, this is the first study on the extension of the BV model using such a framework for analyzing battery data. Furthermore, we are not aware of any studies using the κ -exponential function to do so.

The rest of the manuscript is organized as follows. We provide a brief summary of some important deformed functions (mostly deformed exponential functions) and their properties, and formulate the corresponding modified BV expressions. Then, we analyze experimental lithium battery results compiled from the literature for which we compare fittings using standard and q-and κ -deformed BV equations.

THEORY

Motivation. We consider the simplified case model of an electrode/electrolyte system with a single-step charge transfer redox reaction as described by reaction 2. The global equilibrium of the reacting system, which is driven away from equilibrium, is assumed to be influenced by fluctuations and stochastic events. Such fluctuations can originate, for instance, from the effects of the nonuniformity of the electrode/ electrolyte interfaces, porous and fractal structures, long-range interactions, irreversibilities and parasitic reactions, particle trapping and partial charge transfer, as well as local variations in thermodynamic parameters. When modeling such stochastic dynamics, the question that comes first is how to approximate the noise distribution? This can be modeled on one hand using non-Gaussian distributions when fluctuations are known to display heavy tails and skewness such as in the form of Levystable distributions,²⁹ or on the other hand, the underlying stochastic process can be interpreted as a superposition of multiple Gaussian distributions, leading to the framework of Beck and Cohen superstatistics, 11-13,29 which is also able to explain heavy tails and skewness. We consider here the latter with the assumption that the macroscopic electrode/electrolyte system is made up of many subsystems that are temporarily in local equilibrium, but each has different statistics (e.g., standard deviation). This can also be viewed from the angle in which the process finds an equilibrium with an approximately Gaussian distribution determined by the current noise, and then after a lapse of time large enough compared with the intrinsic time scale

of the system, the system finds another equilibrium also following an approximately Gaussian distribution but with different statistics. In other words, we are considering the situation in which the total distribution of the transfer reaction rate can be viewed as several aggregated Gaussian distributions, making it dependent not only on the potential and absolute temperature as is the case in eqs 6 and 7, but also on the extent and statistics of fluctuations superposed on the equilibrium. The fluctuating variable could be for instance the inverse temperature $\beta=1/T$ (or in energy units $\beta=1/(k_bT)$) or any other intensive quantity. 11,13

In Figure 1, we show a schematic illustration of how one can imagine the inhomogeneous electrode system to look like when discretized into a number of spatial cells with different values of β . Each cell is large enough so that it can be represented by a constant value of β , and thus a single Boltzmann factor is valid. In this regard, from Beck and Cohen, ^{13,46} a generalized Boltzmann factor for the whole system can be written as the integral over all possible fluctuating inverse temperatures β of Boltzmann factors $\exp(-\beta E)$ as

$$B(E) = \int_0^\infty f(\beta) \exp(-\beta E) d\beta$$
 (12)

where $f(\beta)$ represents a normalized probability distribution function (PDF, with $\int_{-\infty}^{\infty} f(\beta) \, \mathrm{d}\beta = 1$) and provides a weight for the distributions $\exp(-\beta E)$. 13 B(E) in eq 12 is essentially the Laplace transform of the function $f(\beta)$, 46 and $f(\beta)$ is here to reshape the Boltzmann distribution into a generalized Boltzmann distribution by providing a statistics for the BG theory statistics, and thus superstatistics of Beck and Cohen. In other words, eq 12 can be used to describe a macroscopic nonequilibrium system in a stationary state (such as the case of electrified electrode/electrolyte system), but locally, the system shall remain infinitely close to equilibrium for which the theory of equilibrium statistical mechanics holds. 47

q-Deformed BV Model. Considering the generalized Boltzmann factor given by eq 12, we now derive an extension to the traditional Boltzmann exponential behavior depending on the choice of the density function $f(\beta)$. Particularly, it is known that the sum of n independent exponentially distributed variables of PDF equal to $a \exp(-a\beta)$ where a > 0 has the discrete PDF: ⁴⁸

$$f_n(\beta) = \frac{a^n}{\Gamma(n)} \beta^{n-1} \exp(-a\beta)$$
(13)

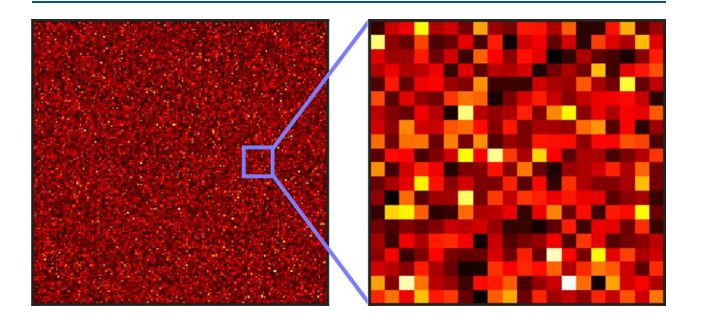


Figure 1. Illustration of a discretized electrode system into a number of spatial cells with different values of inverse temperatures β (derived in this example from a Gamma distribution with unit scale and shape parameter 3). On the left side, we show a low magnification of the electrode, whereas on the right side, a zoomed area is depicted.

By replacing n in eq 13 by any real positive number, we get the general (continuous) Gamma distribution. ⁴⁹ For the case of n =1, one retrieves the exponential distribution, but a number of other distributions can be obtained as special cases, such as the χ -square, Weibull, hydrograph, Rayleigh, or the Maxwell molecular velocity distributions.⁴⁹ This makes the Gamma distribution versatile enough to describe different types of statistics.⁴⁶ We mention that a further generalization of the Gamma distribution (associated with a Bessel function for instance) can be written as⁵⁰

$$f_b(\beta) = \frac{a^{\gamma}}{\Gamma(\gamma) \exp(x/a)} \beta^{\gamma - 1} \exp(-a\beta)_0 F_1(; \gamma; \beta x)$$
(14)

where $\beta > 0$, $\gamma > 0$, a > 0, and ${}_{0}F_{1}(; \gamma; \beta x) = \sum_{0}^{\infty} (\beta x)^{k}/(\gamma)_{k}k!$, $(\gamma)_{k}$ is the Pochhammer symbol $((\gamma)_k = \gamma(\gamma + 1) \cdots (\gamma + k - 1), \gamma \neq 0,$ $(\gamma)_0 = 1$). It is clear that eq 14 with x = 0 reduces to the distribution:

$$f_q(\beta) = \frac{1}{b\Gamma(c)} (\beta/b)^{c-1} \exp(-\beta/b)$$
(15)

in which we used Beck and Cohen's notations 13 where c and bare positive parameters. The integration over $d\beta$ in eq 12 with $f(\beta)$ given by eq 15 leads unambiguously to the closed-form power-law function: 13

$$B(E) = (1 + bE)^{-c} \tag{16}$$

With the substitutions -1/(1-q) = c and $\beta_0 = \int_0^\infty \beta f_q(\beta) d\beta = bc$ being the average of the fluctuating β , the right-hand side of eq 16 is rewritten as 13,32

$$(1 + bE)^{-c} = [1 - (1 - q)\beta_0 E]^{1/(1-q)} \equiv \exp_q(-\beta_0 E)$$
(17)

where $\exp_a(y)$ denotes the q-exponential function parametrized with the real number q. Because c > 0 in the Gamma distribution function (eq 15), q has to be >1 in eq 17, but it can be rewritten with the change of variable q = 2 - q' in order to consider the cases where q' < 1. So, 51 Thus, a generalized Boltzmann factor associated with the Gamma PDF (eq 15) is defined as 13,33,52

$$B_q(E) = \exp_q(-\beta_0 E) \tag{18}$$

The parameter q can be thought of as a characteristic of the system's statistics and is defined here by the ratio of standard variation and the mean of the distribution $f_q(\beta)$, ¹³ noting that when q = 1 there are no superposed fluctuations, and as it should be, the traditional exponential factor is recovered. Alternatively, the ordinary statistics are recovered in the limit $f_q(\beta) \to \delta(\beta - \beta)$ β_0) in eq 12.

We note some of the properties of the q-exponential function: 13,23,46,52

- for q < 1, $\exp_q(y) = 0$ for y < -1/(1-q) and $\exp_q(y) = [1 + (1-q)y]^{1/(1-q)}$ for $y \ge -1/(1-q)$
- for q = 1, $\exp_q(y) = \exp(y)$ for $\forall y$ for q > 1, $\exp_q(y) = [1 + (1 q)y]^{1/(1 q)}$ for y < 1/(q 1)

Figure 2 shows plots of the deformed $\exp_q(-y)$ as a function of y for different values of the parameter q. The usual exponential function is also shown for reference. The logarithm of $\exp_a(-y)$ provided in the same figure shows a linear relationship with y only as $q \rightarrow 1$; otherwise, for q < 1 the curve is convex, and for q > 1 it is concave. ^{44,45,54} In addition to these algebraic properties, the function $\exp_a(-y)$ satisfies the anomalous power-law rate equation $dy/dx = -y^q$ with $q \ne 1$.^{37,55}

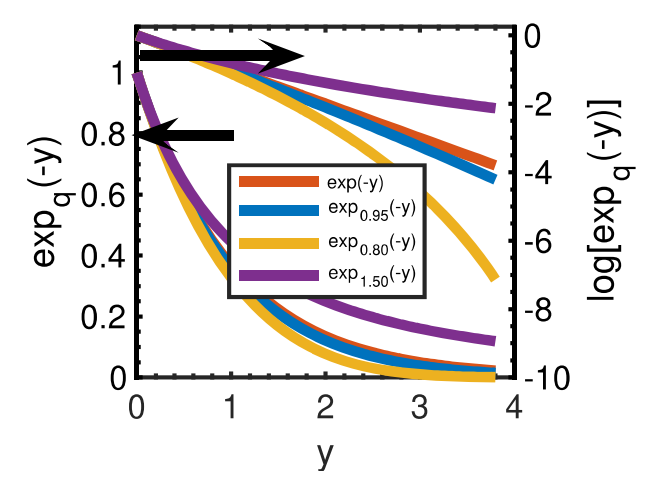


Figure 2. Plots of $\exp(-y)$ and $\exp_q(-y)$ (eq 17) for different values of the parameter q as a function of y.

Another important remark on the q-exponential and the q-Gaussian distributions is that they are the functions associated with some systems showing quasi-stationary states and are the maximizing distributions for the nonadditive Tsallis entropy given by 32,52,56,5

$$S_q = -k \sum_i p_i^q \ln_q(p_i) \tag{19}$$

where k is a positive constant, $q \neq 1$ (also known as the entropic index), and the quantities $p_i = p(E_i)$ represent the probabilities for the occurrence of the *i*th microstate and satisfy $\sum_{i} p_{i} = 1$. The function

$$\ln_{q}(y) = \frac{y^{(1-q)} - 1}{1 - q} \quad (y > 0)$$
(20)

denotes the q-logarithm, the inverse of the q-exponential, i.e., $\ln_a[\exp_a(y)] = \exp_a[\ln_a(y)] = y.^{57}$ In this case, the underlying mathematical mechanism is now the generalized CLT.⁵⁸ It is clear that in the limiting case of $q \to 1$, $\ln_q(y) \to \ln(y)$, and one recovers the standard BG entropy $S_1 = -k_b \sum_i p_i \ln(p_i)$ where k = $k_{\rm b}$ is the Boltzmann constant.³

Finally, the generalized q-deformed BV model we propose, and incorporating the power-law distribution given by the qexponential function for describing the charge transfer reaction rate dependence on the overpotential and temperature, is given

$$i_*^q = [1 - (1 - q)(-\alpha \eta^*)]^{1/(1-q)} - [1 - (1 - q)(1 - \alpha)\eta^*]^{1/(1-q)}$$
(21)

$$=\exp_{q}[-\alpha\eta^{*}] - \exp_{q}[(1-\alpha)\eta^{*}]$$
(22)

We assumed that the parameter q is the same for both halfreactions. Again, recovering the ordinary expression of BV (eq 10) is obtained at the limit $q \to 1$. Furthermore, using the expansion of the q-exponential function for sufficiently small $\exp_{q}(-y) = \exp(-y) \left[1 + \frac{1}{2}(q-1)y^{2} - \frac{1}{3}(q-1)^{2}y^{3}, \right]$

$$+ \dots \Big]$$

one can also recover the usual BV model.¹³

 κ -Deformed BV Model. In the same way used for the formulation of the q-deformed BV model, we propose the following κ -deformed BV model:

$$i_*^{\kappa} = \exp_{\kappa}[-\alpha \eta^*] - \exp_{\kappa}[(1-\alpha)\eta^*]$$
 (23)

where the κ -deformed exponential function of y is given by 34

$$\exp_{\kappa}(y) \equiv \left(\sqrt{1 + \kappa^2 y^2} + \kappa y\right)^{1/\kappa} = \exp\left[\frac{1}{\kappa}\sinh^{-1}(\kappa y)\right]$$
(24)

with $0 \le \kappa < 1$. The function exp (y) emerges from a continuous linear combination of an infinity of standard exponentials as³⁵

$$\exp_{\kappa}(-\beta_0 E) = \int_0^{\infty} \frac{1}{\kappa \beta} J_{1/\kappa} \left(\frac{\beta}{\kappa \beta_0} \right) \exp(-\beta E) d\beta$$
(25)

where $J_{\nu}(y)$ is the Bessel function of the first kind. This is equivalent to how the Gamma distribution is the weight function in the generalized Boltzmann factor given by eq 12 that led to the q-exponential function. Some of the basic properties of $\exp_{x}(y)$

- $\exp_{\kappa \to 0}(y) = \exp(y)$ and $\exp_{\kappa}(y \to 0) = \exp(y)$ ($\exp_{\kappa}(0) = \exp(y)$)
- $\exp_{\kappa}(y) = \exp_{-\kappa}(y)$ for $y \to \infty$, $\exp_{\kappa}(-y)$ is $\sim (2\kappa y)^{-1/\kappa}$ and $\exp_{\kappa}(y) = +\infty$

Its associated inverse function is the κ -logarithm:

$$\ln_{\kappa}(y) = \frac{1}{\kappa} \sinh(\kappa \ln(y)) = \frac{y^{\kappa} - y^{-\kappa}}{2\kappa}$$
(26)

giving $\ln_{\kappa}(\exp_{\kappa}(y)) = \exp_{\kappa}(\ln_{\kappa}(y)) = y$. Kaniadakis' entropy associated with the κ -statistics is obtained by replacing the logarithm in the expression for the standard BG entropy by the κ -logarithm. ^{34,35,59,60}

Plots of the standard $\exp(-y)$ vs $\exp(-y)$ for different values of the parameter κ are provided in Figure 3.

RESULTS AND DISCUSSION

In Figure 4, we show the Tafel plots of electrochemical measurements carried out on a single carbon-coated LiFePO4 particle as-is (i.e., in noncomposite structure without interference from the effect of binders and/or other additive conducting

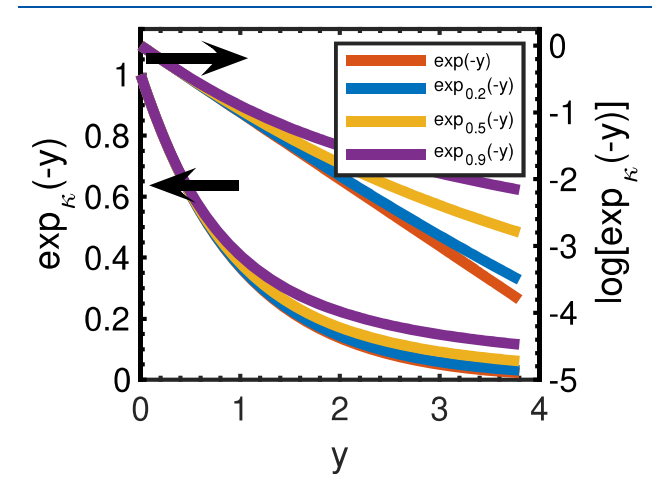


Figure 3. Plots of $\exp(-y)$ and $\exp(-y)$ (eq 24) for different values of κ as a function of y.

materials) from Munakata et al.²⁵ and as adjusted by Bai and Bazant (avoiding concentration polarization effects). Values of current in this single particle technique are usually very small, which makes it acceptable to neglect the ohmic iR drop. Lowmagnification SEM of the target LiFePO₄ particle (see Figure 2 in ref 25) shows that it is spherical in shape, of about 24 μ m in diameter, and consists of agglomerates of many 100 to 200-nmsized primary particles with interparticle porosity and some defects. The specific capacity of the particle was estimated to be 1.5 nA h, and the discharge current used was 750 nA, which took just 4 s for full discharge, i.e., 900 C.²⁵ From the figure, ln(i) vs the (normalized) voltage drop is clearly curved and not as expected for traditional Tafel plots. This convex deviation from linearity was attributed by Munakata et al.²⁵ to the distributions of electric potential and current density, and also to the distribution of Li+ concentration within the porous single particle electrode during charging and discharging, which is usually not observed when nonporous flat electrodes are considered. This nonlinear behavior becomes more significant when high rates are applied, which can be further explained as follows. Let us consider the discharge scheme consisting of the steps (i) Li⁺ diffusion from the bulk electrolyte to the particle surface, followed by (ii) charge transfer at the particle/ electrolyte interface, and then (iii) slow solid-phase diffusion of Li⁺ or polaron diffusion from the surface to the center of the particle coupled with phase transition from FePO₄ to LiFe-PO₄. 25 Step (iii) is the determining step if there is a large spatial gradient of Li⁺ concentration within the particle from surface to center which happens at high discharge current rates, whereas step (ii) may become the controlling step when low rates are applied. In other words, the system can be viewed as a combination of a spectrum of superposed kinetic processes of different origins on the electrode/electrolyte system. If the constituting subsystems are assumed to be temporarily in local equilibrium and follow Boltzmann exponential profiles with different statistics, the system can then be well described with the modified BV models as discussed above.

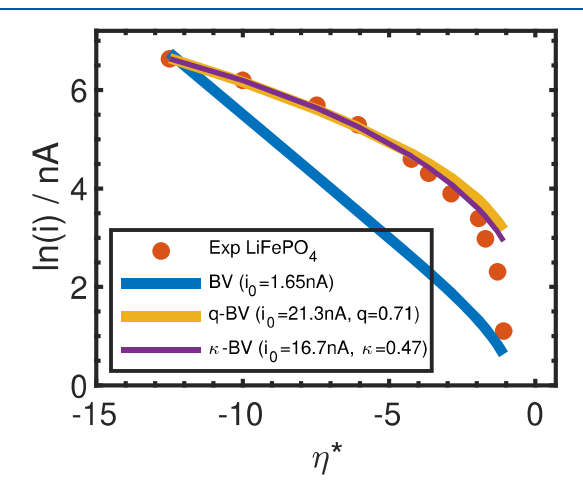


Figure 4. Tafel plots of experimental data by Munakata et al. 1,25 conducted on single carbon-coated LiFePO₄ secondary particle (porous with 24 μ m diameter); the potential drop is originally measured with respect to Li/Li⁺ but is shown here in dimensionless form as done by Bai and Bazant. We also show data fitting with the standard BV model (eq 10), the q-deformed BV model (eq 22), and the κ -deformed BV model (eq 23) with the symmetry factor α set to 0.5.

In the same Figure 4, we show the fitting curves performed with eq 22 (q-BV model), eq 23 (κ -BV model), and eq 10 (standard BV model) with α = 0.5. We used the MATLAB R2019b lsqcurvefit function for nonlinear curve-fitting in the least-squares sense with the same fitting constraints and tolerances for all models for fair comparison. When considering the traditional BV model, the data are poorly fitted with a straight line in the semilogarithmic plane of ln(i) vs η^* , noting that a better fit can be obtained if a smaller portion of the data is selected closer to $\eta^* = 0$ (not shown here; see ref 1). The goodness-of-fit using the normalized root-mean-square error (NRMSE) as the cost function is found to be 0.48, knowing that a value of 1 indicates a perfect fit to the data and $-\infty$ a bad one. The BV model cannot be justified here given the inhomogeneous morphological structure of the electrode as described in ref 25. From the fitting with the q-exponential and κ -exponential modified BV models, however, it is clear that the curved behavior of the data is closely captured. Convex or concave curvatures can be realized depending on the value of the parameter q for the q-deformed model as shown in Figure 2. Here, we found the best fit to be with q = 0.71 < 1.00, which phenomenologically indicates the extent of the system's departure from BG statistics and the associated assumption of thermodynamic equilibrium. Given that in eq 15, c = 1/(q-1)and $b = \beta_0(q - 1)$ (β_0 being the average of the fluctuating β) with q < 1, one can construct the gamma PDF that describes the distribution of fluctuating β in the system. For the κ -deformed BV model we obtained $\kappa = 0.47$, which can also be interpreted in a same way, i.e., the extent of the deviation or dispersion of the data from the usual exponential-based BV model that we can retrieve when $\kappa \to 0$. The values of the prefactor current exchange densities are $i_0 = 21.3$ nA and $i_0 = 16.7$ nA for the q- and κ -deformed models, respectively. The NRMSE fitness values are 0.93 and 0.96, respectively, which are very close to 1. The fittings by both models are very close to each other given the power-law asymptotic behavior of both deformed functions at the relatively large values of the input overpotential. Thus, we are not in the measure to promote or discriminate any of the two without enough information about the local statistics of the electrode/ electrolyte interface.

We note also that the fits are in close agreement with Bai and Bazant's results based on the MHC microscopic theory. The MHC rate is, however, expressed in terms of indefinite integrals of a Gaussian distribution (which includes in its argument an extra term representing a reorganization energy) with Fermi-Dirac statistics of electron energies distributed around the electrode potential. Nonetheless, simple approximations, such as those of Zeng et al.⁶ using asymptotic analysis methods, have shown very good agreement with the experiments which should make the MHC framework more attractive from a computational point-of-view. On the other hand, both of the deformed BV models are also the results of superimposed statistics obtained from integral transforms of superimposed density on another density, provide exact closed-form expressions, and are simple and easy to implement with comparable accuracy and fitting capabilities. They can be viewed as macroscopic models providing a posteriori (statistical) information about the inhomogeneity of the system at the level of subcells, which is encoded in the PDF $f(\beta)$.

The curvature of the Tafel plots for other materials and systems may be different, which can still be captured by the free parameters q or κ depending on the model as shown in Figure 5. The figure depicts the experimental Tafel plots extracted from

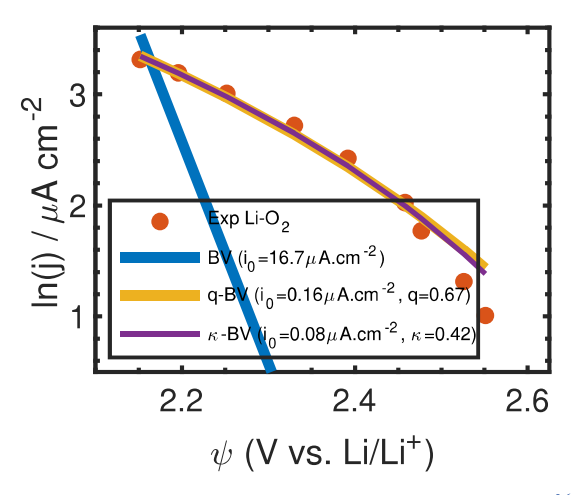


Figure 5. Tafel plots of experimental data by Viswanathan et al. ²⁶ for the discharge of the Li–O₂ battery. We also show data fitting with the standard BV model (eq 9), q-deformed BV model (eq 22), and κ -BV model (eq 23) with the symmetry factor α = 0.5.

Viswanathan et al.²⁶ for the discharge of Li–air (or Li–O₂) battery. The net reaction is $2\text{Li} + \text{O}_2 \rightleftharpoons \text{Li}_2\text{O}_2$ with the battery discharge described by the forward direction. The nonlinear curve has been attributed to a complex crystal growth and dissolution mechanism of Li_2O_2 which can occur on different crystal facets or terminations on the electrode or on different sites (terrace, step or kink), and could involve different combinations of nucleation and diffusion²⁶ or other mechanisms.²¹ From the figure, it is clear that the standard BV model also fails to adequately fit these types of data, whereas based on different statistics than BG theory, the q- and κ -deformed BV models nicely followed the trend of the curve with (q = 0.67, $i_0 = 0.16~\mu\text{A}$ cm⁻²) and ($\kappa = 0.42$, $i_0 = 0.08~\mu\text{A}$ cm⁻²), respectively. The goodness-of-fit between the models and the experimental data are -0.11, 0.89, and 0.91, respectively.

CONCLUSION

In this contribution, we proposed and verified the application of two deformed versions of the BV model for the analysis of convex semilogarithmic current-overpotential profiles observed with some battery data. The models assume that the nonequilibrium electrode/electrolyte system can be viewed as a multitude of subsystems temporarily in local equilibrium, and thus follow the Boltzmann exponential trend only locally and with different statistics. These fluctuations are taken to be inverse temperature fluctuations that can be correlated for instance to spatial inhomogeneities of the interface geometry, long-range interactions, particle trapping, and partial charge transfer, as well as distribution of thermodynamic quantities. Applied to two different examples of battery data, 1,25,26 both deformed models with only one free parameter each (based on the q- or κ -exponential functions) showed very close agreement with the experiments. The extra degree of freedom in the modified BV models is related to the extent of deviation of the data from BG statistics assumed in classical BV, which itself can be retrieved when $q \to 1$ in eq 22 or $\kappa \to 0$ in eq 23. The deformed BV models can be applied in principle to other types of usual or unusual reaction data and power-law relaxation behavior found in corrosion reactions, sensors, electrocatalytic processes, solar cells, etc.

AUTHOR INFORMATION

Corresponding Author

Anis Allagui — Department of Sustainable and Renewable Energy Engineering and Center for Advanced Materials Research, Research Institute of Sciences and Engineering, University of Sharjah, Sharjah, United Arab Emirates; Department of Mechanical and Materials Engineering, Florida International University, Miami, Florida 33174, United States; orcid.org/0000-0001-6044-9158; Email: aallagui@sharjah.ac.ae

Authors

Hachemi Benaoum — Department of Applied Physics and Astronomy, University of Sharjah, Sharjah, United Arab Emirates

Chunlei Wang — Department of Mechanical and Materials Engineering, Florida International University, Miami, Florida 33174, United States; occid.org/0000-0003-2574-7314

Complete contact information is available at: https://pubs.acs.org/10.1021/acs.jpcc.1c09620

Notes

The authors declare no competing financial interest.

ACKNOWLEDGMENTS

This work is supported by NSF project #2126190 (C.W. and A.A.). We would like to thank the anonymous referees for their valuable comments that improved the quality of the paper.

REFERENCES

- (1) Bai, P.; Bazant, M. Z. Charge transfer kinetics at the solid—solid interface in porous electrodes. *Nat. Commun.* **2014**, *5*, 1–7.
- (2) Dreyer, W.; Guhlke, C.; Müller, R. A new perspective on the electron transfer: recovering the Butler–Volmer equation in non-equilibrium thermodynamics. *Phys. Chem. Chem. Phys.* **2016**, *18*, 24966–24983.
- (3) Marcus, R. A. Symmetry or asymmetry of k_{ET} and i_{STM} vs potential curves. J. Chem. Soc., Faraday Trans. **1996**, 92, 3905.
- (4) Chidsey, C. E. D. Free energy and temperature dependence of electron transfer at the metal-electrolyte interface. *Science* **1991**, *251*, 919.
- (5) Sripad, S.; Korff, D.; DeCaluwe, S. C.; Viswanathan, V. Kinetics of lithium electrodeposition and stripping. *J. Chem. Phys.* **2020**, *153*, 194701.
- (6) Zeng, Y.; Smith, R. B.; Bai, P.; Bazant, M. Z. Simple formula for Marcus—Hush—Chidsey kinetics. *J. Electroanal. Chem.* **2014**, *735*, 77—83.
- (7) Kurchin, R.; Viswanathan, V. Marcus—Hush—Chidsey kinetics at electrode—electrolyte interfaces. *J. Chem. Phys.* **2020**, *153*, 134706.
- (8) Migliore, A.; Nitzan, A. On the evaluation of the Marcus—Hush—Chidsey integral. *J. Electroanal. Chem.* **2012**, *671*, 99—101.
- (9) Migliore, A.; Nitzan, A. Nonlinear charge transport in redox molecular junctions: A Marcus perspective. *ACS Nano* **2011**, *5*, 6669–6685.
- (10) Oldham, K. B.; Myland, J. C. On the evaluation and analysis of the Marcus—Hush—Chidsey integral. *Journal of electroanalytical chemistry* **2011**, 655, 65–72.
- (11) Beck, C. Superstatistics: theory and applications. *Continuum Mech. Thermodyn.* **2004**, *16*, 293–304.
- (12) Abe, S.; Beck, C.; Cohen, E. G. Superstatistics, thermodynamics, and fluctuations. *Phys. Rev. E* **2007**, *76*, No. 031102.
- (13) Beck, C.; Cohen, E. G. Superstatistics. *Physica A* **2003**, 322, 267–275.
- (14) Gutman, E. Empiricism or self-consistent theory in chemical kinetics? *Journal of alloys and compounds* **2007**, 434, 779–782.

- (15) Yang, F. Generalized Butler-Volmer relation on a curved electrode surface under the action of stress. *Sci. China Phys. Mech. Astron.* **2016**, *59*, 1–7.
- (16) Fletcher, S. Tafel slopes from first principles. J. Solid State Electrochem. 2009, 13, 537-549.
- (17) Vetter, K. J. Electrochemical kinetics: theoretical and experimental aspects; Academic Press, 1967.
- (18) Pollak, E.; Talkner, P. Reaction rate theory: What it was, where is it today, and where is it going? *Chaos: An Interdisciplinary Journal of Nonlinear Science* **2005**, *15*, No. 026116.
- (19) Li, D.; Lin, C.; Batchelor-McAuley, C.; Chen, L.; Compton, R. G. Tafel analysis in practice. *J. Electroanal. Chem.* **2018**, 826, 117–124.
- (20) Banham, D. W.; Soderberg, J. N.; Birss, V. I. Pt/carbon catalyst layer microstructural effects on measured and predicted tafel slopes for the oxygen reduction reaction. *J. Phys. Chem. C* **2009**, *113*, 10103—10111.
- (21) Sankarasubramanian, S.; Seo, J.; Mizuno, F.; Singh, N.; Prakash, J. Elucidating the oxygen reduction reaction kinetics and the origins of the anomalous Tafel behavior at the lithium—oxygen cell cathode. *J. Phys. Chem. C* **2017**, *121*, 4789—4798.
- (22) Soderberg, J. N.; Co, A. C.; Sirk, A. H.; Birss, V. I. Impact of porous electrode properties on the electrochemical transfer coefficient. *J. Phys. Chem. B* **2006**, *110*, 10401–10410.
- (23) Allagui, A.; Benaoum, H.; Olendski, O. On the Gouy-Chapman-Stern model of the electrical double-layer structure with a generalized Boltzmann factor. *Physica A* **2021**, *582*, 126252.
- (24) Boyle, D. T.; Kong, X.; Pei, A.; Rudnicki, P. E.; Shi, F.; Huang, W.; Bao, Z.; Qin, J.; Cui, Y. Transient voltammetry with ultramicroelectrodes reveals the electron transfer kinetics of lithium metal anodes. *ACS Energy Letters* **2020**, *5*, 701–709.
- (25) Munakata, H.; Takemura, B.; Saito, T.; Kanamura, K. Evaluation of real performance of LiFePO4 by using single particle technique. *J. Power Sources* **2012**, *217*, 444–448.
- (26) Viswanathan, V.; Nørskov, J.; Speidel, A.; Scheffler, R.; Gowda, S.; Luntz, A. Li–O2 kinetic overpotentials: Tafel plots from experiment and first-principles theory. *journal of physical chemistry letters* **2013**, *4*, 556–560.
- (27) Yin, C.; Du, J. The collision theory reaction rate coefficient for power-law distributions. *Physica A: Statistical Mechanics and its Applications* **2014**, 407, 119–127.
- (28) Claycomb, J.; Nawarathna, D.; Vajrala, V.; Miller, J., Jr Power law behavior in chemical reactions. *J. Chem. Phys.* **2004**, *121*, 12428–12430.
- (29) Schäfer, B.; Beck, C.; Aihara, K.; Witthaut, D.; Timme, M. Non-Gaussian power grid frequency fluctuations characterized by Lévystable laws and superstatistics. *Nature Energy* **2018**, *3*, 119–126.
- (30) Kaniadakis, G.; Baldi, M. M.; Deisboeck, T. S.; Grisolia, G.; Hristopulos, D. T.; Scarfone, A. M.; Sparavigna, A.; Wada, T.; Lucia, U. The κ-statistics approach to epidemiology. *Sci. Rep.* **2020**, *10*, 1–14.
- (31) Zhang, W.; Wang, X.; Kong, Q.; Ruan, H.; Zuo, X.; Ren, Y.; Cao, Q.; Wang, H.; Zhang, D.; Jiang, J. Power–Law Feature of Structure in Metallic Glasses. *J. Phys. Chem. C* 2019, 123, 27868–27874.
- (32) Tsallis, C. Possible generalization of Boltzmann-Gibbs statistics. *J. Stat. Phys.* **1988**, 52, 479–487.
- (33) Tsallis, C. Beyond Boltzmann-Gibbs-Shannon in Physics and Elsewhere. *Entropy* **2019**, *21*, 696.
- (34) Kaniadakis, G. Non-linear kinetics underlying generalized statistics. *Physica A: Statistical mechanics and its applications* **2001**, 296, 405–425.
- (35) Kaniadakis, G. Theoretical foundations and mathematical formalism of the power-law tailed statistical distributions. *Entropy* **2013**, *15*, 3983–4010.
- (36) Lenzi, E.; Anteneodo, C.; Borland, L. Escape time in anomalous diffusive media. *Phys. Rev. E* **2001**, *63*, No. 051109.
- (37) Niven, R. K. q-Exponential structure of arbitrary-order reaction kinetics. *Chem. Eng. Sci.* **2006**, *61*, 3785–3790.
- (38) Bağcı, G. Nonextensive reaction rate. *Physica A: Statistical Mechanics and its Applications* **2007**, 386, 79–84.

- (39) Yin, C.; Du, J. The power-law reaction rate coefficient for an elementary bimolecular reaction. *Physica A: Statistical Mechanics and its Applications* **2014**, 395, 416–424.
- (40) Yin, C.; Guo, R.; Du, J. The rate coefficients of unimolecular reactions in the systems with power-law distributions. *Physica A: Statistical Mechanics and its Applications* **2014**, 408, 85–95.
- (41) Cangtao, Y.; Du, J. The power-law reaction rate coefficient for barrierless reactions. *Journal of Statistical Mechanics: Theory and Experiment* **2014**, 2014, P07012.
- (42) Aquilanti, V.; Mundim, K. C.; Elango, M.; Kleijn, S.; Kasai, T. Temperature dependence of chemical and biophysical rate processes: Phenomenological approach to deviations from Arrhenius law. *Chem. Phys. Lett.* **2010**, 498, 209–213.
- (43) Quapp, W.; Zech, A. Transition state theory with Tsallis statistics. *Journal of computational chemistry* **2009**, 31, 573–585.
- (44) Silva, V. H.; Aquilanti, V.; de Oliveira, H. C.; Mundim, K. C. Uniform description of non-Arrhenius temperature dependence of reaction rates, and a heuristic criterion for quantum tunneling vs classical non-extensive distribution. *Chem. Phys. Lett.* **2013**, 590, 201–207.
- (45) Aquilanti, V.; Coutinho, N. D.; Carvalho-Silva, V. H. Kinetics of low-temperature transitions and a reaction rate theory from non-equilibrium distributions. *Philosophical Transactions of the Royal Society A: Mathematical, Physical and Engineering Sciences* **2017**, 375, 20160201.
- (46) Beck, C. Stretched exponentials from superstatistics. *Physica A: Statistical Mechanics and its Applications* **2006**, 365, 96–101.
- (47) Ourabah, K. Fingerprints of nonequilibrium stationary distributions in dispersion relations. *Sci. Rep.* **2021**, *11*, 1–13.
- (48) Bondesson, L. Generalized gamma convolutions and related classes of distributions and densities; Springer Science & Business Media, 2012; Vol. 76.
- (49) Lienhard, J. H.; Meyer, P. L. A physical basis for the generalized gamma distribution. *Quarterly of Applied Mathematics* **1967**, 25, 330–334.
- (50) Sebastian, N. A generalized gamma model associated with a Bessel function. *Integral transforms and Special functions* **2011**, 22, 631–645.
- (51) Wilk, G.; Włodarczyk, Z. Consequences of temperature fluctuations in observables measured in high-energy collisions. *European Physical Journal A* **2012**, *48*, 1–13.
- (52) Abe, S.; Okamoto, Y. Nonextensive statistical mechanics and its applications; Springer Science & Business Media, 2001; Vol. 560.
- (53) Borges, E. P. A possible deformed algebra and calculus inspired in nonextensive thermostatistics. *Physica A: Statistical Mechanics and its Applications* **2004**, 340, 95–101.
- (54) Truhlar, D. G.; Kohen, A. Convex Arrhenius plots and their interpretation. *Proc. Natl. Acad. Sci. U. S. A.* **2001**, *98*, 848–851.
- (55) Lyra, M.; Tsallis, C. Nonextensivity and multifractality in low-dimensional dissipative systems. *Phys. Rev. Lett.* **1998**, *80*, 53.
- (56) Tsallis, C. Nonextensive statistics: theoretical, experimental and computational evidences and connections. *Braz. J. Phys.* **1999**, 29, 1–35.
- (57) Tsallis, C. What should a statistical mechanics satisfy to reflect nature? *Physica D* **2004**, *193*, 3–34.
- (58) Umarov, S.; Tsallis, C.; Steinberg, S. On aq-central limit theorem consistent with nonextensive statistical mechanics. *Milan journal of mathematics* **2008**, *76*, 307–328.
- (59) Abreu, E. M.; Neto, J. A.; Mendes, A. C.; Bonilla, A. Tsallis and Kaniadakis statistics from a point of view of the holographic equipartition law. *EPL (Europhysics Letters)* **2018**, *121*, 45002.
- (60) Kaniadakis, G.; Scarfone, A.; Sparavigna, A.; Wada, T. Composition law of κ -entropy for statistically independent systems. *Phys. Rev. E* **2017**, *95*, No. 052112.